ChemComm

COMMUNICATION

View Article Online
View Journal | View Issue

Cite this: *Chem. Commun.*, 2019, 55, 7784

Received 9th May 2019,
Accepted 7th June 2019

DOI: 10.1039/c9cc03441b

rsc.li/chemcomm

Rapid growth of fully-inorganic flexible Ca_xCoO_2 thin films from a ligand free aqueous precursor ink for thermoelectric applications†

Tridib Kumar Sinha,[ab] Jinho Lee,[c] Jin Kuk Kim,[b] Samit K. Ray[ad] and Biplab Paul*[e]

We demonstrate a ligand-free green chemical method for the rapid growth of nanoporous $Ca_{0.35}CoO_2$ thin films on sapphire and mica substrates from a water-based precursor ink, formulated by dissolving the precursor solid, composed of *in situ* prepared Ca^{2+}–DMF and Co^{2+}–DMF complexes. Mica serves as the flexible substrate as well as the sacrificial layer for the film transfer. Despite the presence of nanopores, the power factor of the flexible film $Ca_{0.35}CoO_2$-on-mica is above 0.50 $\times$ 10^{-4} W m^{-1} K^{-2} at around room temperature. The present technique is simple and cost-effective.

Layered calcium cobaltates, *e.g.*, Ca_xCoO_2 and $[Ca_2CoO_3]_{0.62}CoO_2$ (also represented as $Ca_3Co_4O_9$), because of their remarkable thermal and chemical stability and nontoxicity, have attracted significant interest for diverse applications, *e.g.* catalysis,[1,2] batteries,[3] supercapacitors,[4] optoelectronics,[5] and particularly for thermoelectrics.[6–11] The thin films of this class of materials can be promising for flexible applications if film deposition is possible on flexible substrates or otherwise transferable onto flexible platforms. Although, Ca_xCoO_2 thin films have been grown by physical deposition techniques,[12,13] for scalability, chemical solution deposition (CSD) methods are often preferred over the physical methods. In particular, the CSD technique is cost-effective and facile.[14–16] However, oxide materials are mostly insoluble, restricting their solution processability. For $Ca_3Co_4O_9$, sol–gel chemical methods have been implemented, however the poor structural quality, arising from undesired cross-reactions or non-homogeneous precipitation limits its applicability.[17,18] Panchakarla *et al.* reported the growth of misfit layered $Ca_3Co_4O_9$ nanotubes by base-treatment of pre-formulated calcium cobalt oxide,[19] but, because of the insolubility factor, the process seems to be complicated for the deposition of thin films.

There are some methods to formulate the thermoelectric inks but mostly with thermally unstable organic polymers.[14] Because of the availability of suitable solvents, some chalcogenidometallate-based TE materials have been developed from the respective precursor inks,[15] but with no such report on oxide materials. Recently, the growth of misfit layered cobaltate thin films has been accomplished using a water-based solution containing the co-ordination complex of metal ions with EDTA (ethylenediaminetetraacetic acid) and PEI (polyethyleneimine).[20] However, the preparation of the complex-solution remains tedious, time consuming and moreover hazardous.[21,22] Despite some investigations on the CSD growth of $Ca_3Co_4O_9$, there is no report on the growth of Ca_xCoO_2 by this route. The Ca_xCoO_2 thin film, due to its higher power factor compared to $Ca_3Co_4O_9$, is promising for near room temperature TE applications. The $Ca_{0.33}CoO_2$ thin film is reported to exhibit a high power factor of 0.9 mW m^{-1} K^{-2} at 300 K,[23] which is several times higher than that of $Ca_3Co_4O_9$,[8–11] and remarkably higher than those of other layered cobaltates A_xCoO_2 [A = Sr, La, Pr, or Nd].[6,7,24,25] For a high output power from a thermoelectric converter (TEC), its constituent active materials are required to have a high power factor.[26] In fact, having a high power factor is more important than efficiency for a thin film based TEC with planar geometry, where heat flows in parallel to the film surface.[27]

Therefore, the development of alternative strategies to grow high performance and mechanically flexible Ca_xCoO_2 thin films in a facile, cost-effective and environment-friendly process can offer a viable solution for low power requirements of emerging portable and wearable electronics. Here, we report the rapid growth of $Ca_{0.35}CoO_2$ thin films on sapphire and flexible mica substrates from a ligand-free aqueous TE precursor ink. The ink is a mixture of *in situ* prepared Ca^{2+}–DMF and Co^{2+}–DMF complexes. The fully-inorganic flexible $Ca_{0.35}CoO_2$-on-mica film, unlike organic and hybrid films, can sustain high temperature and thus be useful for applications in a wide temperature range:

[a] *Department of Physics, Indian Institute of Technology, Kharagpur 721302, India*
[b] *Department of Materials Engineering and Convergence Technology, Gyeongsang National University, Jinju 52828, South Korea*
[c] *The Research Institute of Natural Science and Department of Physics Education, Gyeongsang National University, Jinju 52828, South Korea*
[d] *S N Bose National Centre for Basic Sciences, Kolkata 700106, India*
[e] *Thin Film Physics Division, Department of Physics, Chemistry, and Biology (IFM), Linköping University, SE-581 83 Linköping, Sweden. E-mail: biplab.paul@liu.se*

† Electronic supplementary information (ESI) available: The details of the synthesis procedures. See DOI: 10.1039/c9cc03441b

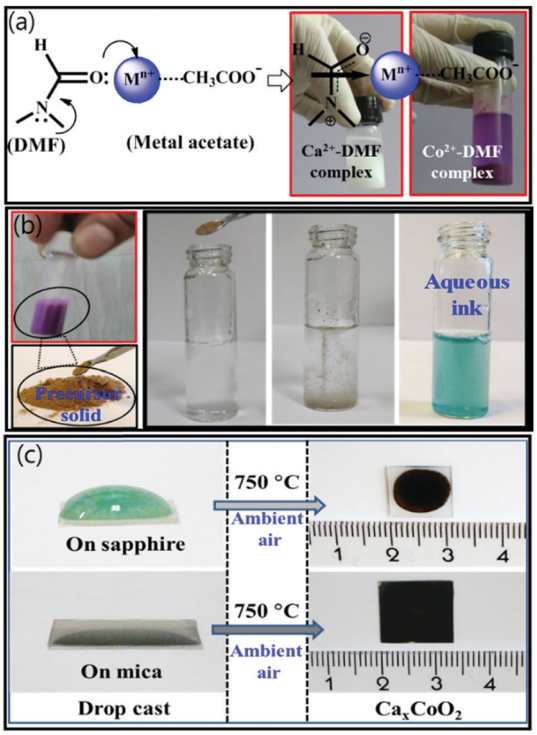

Fig. 1 (a) Formation of the Ca^{2+}–DMF and Co^{2+}–DMF complexes as white and violet precipitates, respectively. (b) Formation of a pink brown precursor solid and the preparation of an aqueous TE ink, (c) the $Ca_{0.35}CoO_2$ thin film on the sapphire and mica substrates, grown by drop casting the ink followed by annealing at 700 °C in air.

from room-temperature wearable applications (harvesting electrical power from body heat to power wearable electronics) to waste-heat recovery from hot surfaces of varying geometries (*e.g.*, hot pipes).

Metal ions such as Ca^{2+}, Co^{2+}, *etc.* are very susceptible to complexation with polar solvents such as DMF.[28–31] DMF is cheaper[31] as well as less-hazardous[32] and recyclable. The white precipitate of Ca^{2+}–DMF and violet precipitate of Co^{2+}–DMF were separately prepared, as shown in Fig. 1a, simply by dissolving the salts (*i.e.*, $Ca(CH_3COO)_2{\cdot}H_2O$ and $Co(CH_3COO)_2{\cdot}H_2O$) in a molar ratio of 3 : 4 into an excess of hot DMF, followed by subsequent cooling at room temperature. The DMF forms complexes with the metal ions through its amide functionality (as schematically shown in Fig. 1a). A purple color precipitate was obtained by mixing the precipitates of Ca^{2+}–DMF and Co^{2+}–DMF, and re-precipitating from the hot DMF, as shown in Fig. 1b, which upon drying, produces a pink brown color precursor solid. This solid was easily dissolved in de-ionized (DI) water to obtain a stable homogenous solution of a bluish precursor ink (Fig. 1b). During the formation of DMF-complexes, there is a possibility of partial substitution of the acetate ions ($-COOCH_3^-$) by the DMF.

The DMF-complexes are likely to behave as zwitterions. During the mixing of the DMF-complexes, the zwitterions electrostatically interact with each other, and form the precipitate of the complex-conjugates, which was dried to obtain the pink brown precursor solid. The solid is likely to be soluble in polar solvents because of its abundant ionic characteristics. Water, being the most environmentally friendly polar solvent, here, we have demonstrated the formulation of a stable (stability was noticed for 60 days) aqueous precursor ink for TE application. The ink (containing a solid content of 10 mg mL^{-1}) was drop-casted on sapphire and mica substrates, as shown in Fig. 1c. The muscovite mica, because of its inherently layered structure, where aluminosilicate layers are loosely bound by the boundary layer of potassium (K^+) ions, can serve as the flexible substrate.[33]

After heat treatment at 700 °C for 10 min under an ambient atmosphere, the precursor solution turned into dark films of $Ca_{0.35}CoO_2$. The film on the mica substrate, unlike that on the sapphire substrate, was uniform. This is because, the angle of contact between the solution and hydrophilic mica[34] is much smaller than that of sapphire, which results in uniform spreading of the solution over the mica substrate.

During the mixing of the DMF-complexes under vigorous stirring, the Co^{2+}–DMF complex (because of its smaller size) occupies the interstitial spaces of Ca^{2+}–DMF through the favorable electrostatic interaction among the active groups in the periphery of the metal ions, resulting in an *in situ* electrically and stoichiometrically balanced thermoelectric precursor solid (*i.e.*, Ca^{2+}/Co^{2+}–DMF mixed complex). During heat treatment, the coordinated DMF reduces the Co^{2+} nanoparticles to Co^0 nanoparticles, which in the presence of abundant oxygen transform to CoO_2.[35,36] The plausible reaction mechanism is shown in Scheme S1 (ESI†). The DMF degrades at high temperature, producing H_2O, CO_2, N_2, NO_x, *etc.*, resulting in porosity in the films. Ca^{2+}–DMF is ionized at high temperature and forms $Ca_{0.35}CoO_2$.

Fig. 2a and b show the XRD scans of the films $Ca_{0.35}CoO_2$-on-mica and $Ca_{0.35}CoO_2$-on-sapphire, respectively. Both the figures show $Ca_{0.35}CoO_2$ 001 and 002 peaks. The peaks from no other planes, except the (00*l*) planes of $Ca_{0.35}CoO_2$, indicate the *c*-axis orientation of both the films. Apart from $Ca_{0.35}CoO_2$, the peaks from the mica and sapphire substrates are also visible as shown in Fig. 2a and b, respectively. The *d*-spacing for both the films is calculated to be 5.437 Å, which nearly matches with the value reported elsewhere.[37]

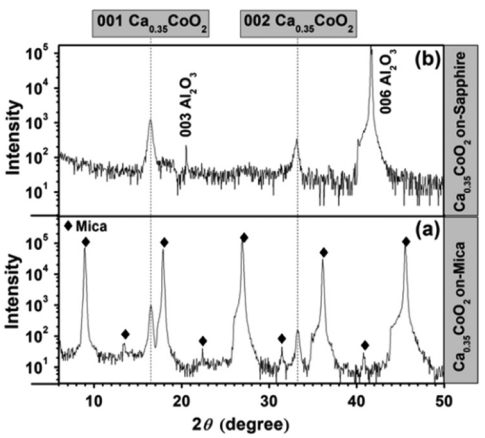

Fig. 2 XRD patterns of the films (a) $Ca_{0.35}CoO_2$-on-mica and (b) $Ca_{0.35}CoO_2$-on-sapphire.

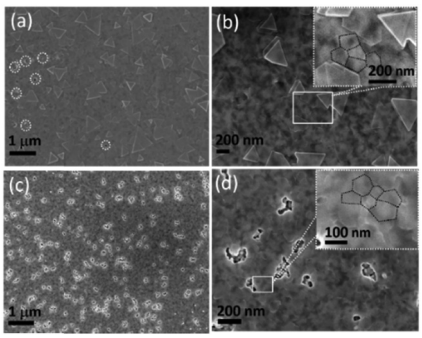

Fig. 3 (a) SEM image of $Ca_{0.35}CoO_2$-on-sapphire. (b) Magnified image of a small portion of the $Ca_{0.35}CoO_2$-on-sapphire film; and the inset shows the polygonal shape of the grains in the film. (c) SEM image of $Ca_{0.35}CoO_2$-on-mica. (d) Magnified image of a small portion of the $Ca_{0.35}CoO_2$-on-mica film; and the inset shows the polygonal shape of the fine grains in the film.

Fig. 3a shows a typical SEM image of $Ca_{0.35}CoO_2$-on-sapphire. A random distribution of the triangular grains of $Ca_{0.35}CoO_2$ is visible in Fig. 3a. The presence of nanopores in the film is indicated by the white open circles. Fig. 3b shows the magnified SEM image. The inset of Fig. 3b shows the polygonal shape of some fine grains of $Ca_{0.35}CoO_2$ of dimension less than 200 nm. Fig. 3c shows a typical SEM image of $Ca_{0.35}CoO_2$-on-mica, where the random distribution of nanopores of irregular shapes is clearly visible. A relatively smooth surface and the absence of any larger grains above 200 nm are evident from the magnified SEM image (Fig. 3d). The inset of Fig. 3d shows the polygonal shape of the grains of $Ca_{0.35}CoO_2$. The seemingly flat surface of both the films is attributed to the out-of-plane orientation of the films, which is consistent with the XRD observation. The growth of oriented films on both the substrates is intrinsically attributed to the effect of self-assembly during annealing, where the driving force is the external stress due to solvent evaporation.[38] The higher porosity of $Ca_{0.35}CoO_2$-on-mica compared to $Ca_{0.35}CoO_2$-on-sapphire might be due to the slow evaporation of the surface absorbed water in the more hygroscopic mica during the formation of the film.[39] From the above study, it is conjectured that the present CSD method can be applicable to grow $Ca_{0.35}CoO_2$ thin films on arbitrary substrates, which sustain a high annealing temperature of 700 °C. The porosity of the films can also be controlled by preferential selection of the substrate with the desired hygroscopic properties.

Fig. 4a shows a typical optical image of the bent $Ca_{0.35}CoO_2$ film of thickness ~300 nm on the mica substrate (25 μm thickness). The film is bendable to a bending radius of 15 mm without developing any cracks, as confirmed by optical microscopy. As shown in Fig. 4b, the transferability of the film is demonstrated by transferring the film from the parent mica substrate onto a sticky tape.

Fig. 5a shows the temperature dependent electrical resistivity of $Ca_{0.35}CoO_2$-on-sapphire (red circles) and $Ca_{0.35}CoO_2$-on-mica (black open circles). The room temperature resistivity values are 15.6 and 14.6 mΩ cm for $Ca_{0.35}CoO_2$-on-sapphire and $Ca_{0.35}CoO_2$-on-mica, respectively, which are higher than

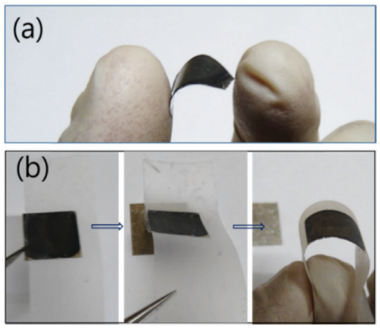

Fig. 4 (a) Image of thin flexible $Ca_{0.35}CoO_2$-on-mica film. (b) Demonstration of the film transfer onto sticky tape.

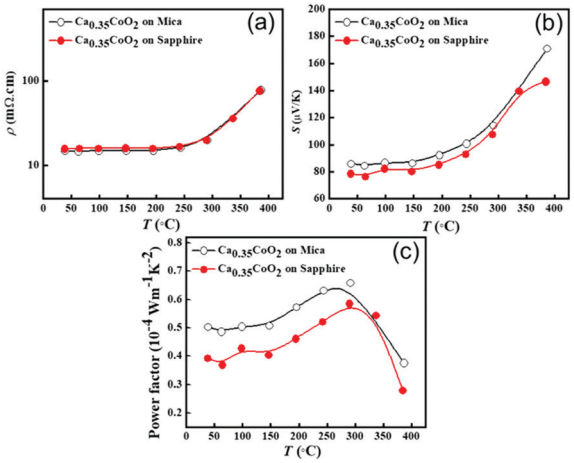

Fig. 5 Temperature dependent (a) electrical resistivity, (b) Seebeck coefficient, and (c) power factor of the films $Ca_{0.35}CoO_2$-on-mica and $Ca_{0.35}CoO_2$-on-sapphire.

the values for $Ca_{0.35}CoO_2$ reported elsewhere,[12,40] however, comparable to that of undoped $Ca_3Co_4O_9$ thin films.[41,42] Even with a nanoporous structure, the low electrical resistivity of $Ca_{0.35}CoO_2$-on-mica is attributed to its better crystalline quality than the film $Ca_{0.35}CoO_2$-on-sapphire. From this, it is apparent that the nanopores do not act as the scattering centre for the charge carriers, which might be due to the greater interpore separation compared to the electron mean free path. However, the thermal conductivity of the film is anticipated to be reduced, due to the enhanced scattering of phonons by the nanopores. This anticipation is due to the fact that the phonon mean free path is one order of magnitude higher than the electron mean free path, and by controlling the characteristic length scale of the nanoporous structure within the range of electron and phonon mean free paths, the phonons can be selectively scattered, but without hampering the electronic transport.[43,44] Fig. 5b shows the temperature dependent Seebeck coefficient of the films. The room temperature Seebeck coefficient values are 78 and 88 μV K^{-1} for the $Ca_{0.35}CoO_2$-on-sapphire and $Ca_{0.35}CoO_2$-on-mica films, respectively, which are comparable to the value reported for single crystalline $Ca_{0.33}CoO_2$,[30] however, sufficiently higher than those of sputter deposited Ca_xCoO_2 thin films reported elsewhere.[15] The Seebeck

coefficient varies with temperature in a similar manner to the electrical resistivity. Fig. 5c shows the temperature dependent power factor of the films. The room temperature power factor values are 0.39 and 0.50 $\times$ 10^{-4} W m^{-1} K^{-2} for the films $Ca_{0.35}CoO_2$-on-sapphire and $Ca_{0.35}CoO_2$-on-mica, respectively, which are interestingly comparable to the reported values for undoped $Ca_3Co_4O_9$ thin films.[41,42] The slightly higher power factor of the film $Ca_{0.35}CoO_2$-on-mica compared to that of the $Ca_{0.35}CoO_2$-on-sapphire film is attributed to the lower electrical resistivity of the former than the latter.

The film $Ca_{0.35}CoO_2$-on-mica can be useful for flexible applications in a wide temperature range, from room temperature to a few hundred degrees above room temperature, due to its high power factor, above 0.50 $\times$ 10^{-4} W m^{-1} K^{-2} until 300 °C. To investigate the effect of bending stress on the TE performance, the $Ca_{0.35}CoO_2$-on-mica film was subjected to 100 times of bending, and then TE measurements were performed. No notable changes in the Seebeck coefficient and electrical resistivity values were found; and any small variations in the values are within the error limit specified for the measuring instrument. It is noteworthy that the present films are undoped and a further improvement of the power factor is still possible upon doping.

The present thin film growth technique from the thermoelectric precursor ink, being simple, eco-friendly and less time consuming, is potentially suitable for industrial upscaling.

This research was supported by the Science and Engineering Research Board (SERB/1759/2014-15), the DST "GPU", Government of India, Basic Science Research Program through the National Research Foundation of Korea (NRF) funded by the Ministry of Education (2016R1D1A1B03931391), and through funding from the Åforsk foundation (Grant No. 17-578). P. Eklund (Linköping University) is acknowledged for his critical reading of the manuscript and additional funding through the Swedish Government Strategic Research Area in Materials Science on Functional Materials at Linköping University (Faculty Grant SFO-Mat-LiU No. 2009 00971).

Conflicts of interest

There are no conflicts to declare.

References

1 C. Dang, Y. Li, S. M. Yusuf, Y. Cao, H. Wang, H. Yu, F. Peng and F. Li, *Energy Environ. Sci.*, 2018, **11**(3), 660–668.
2 C. S. Lim, C. K. Chua, Z. Sofer, O. Jankovsky and M. Pumera, *Chem. Mater.*, 2014, **26**(14), 4130–4136.
3 D. W. Kim, Y. D. Ko, J. G. Park and B. K. Kim, *Angew. Chem.*, 2007, **46**(35), 6654–6657.
4 Z. Wang, Y. Wang, X. Yue, G. Shi, M. Shang, Y. Zhang, Z. Lv and G. Ao, *J. Alloys Compd.*, 2019, **792**, 357–364.
5 L. Lajaunie, A. Ramasubramaniam, L. S. Panchakarla and R. Arenal, *Appl. Phys. Lett.*, 2018, **113**(3), 031102.
6 G. G. Yadav, A. David, T. Favaloro, H. Yang, A. Shakouri, J. Caruthers and Y. Wu, *J. Mater. Chem. A*, 2013, **1**(38), 11901–11908.
7 V. Thoréton, Y. Hu, C. Pirovano, E. Capoen, N. Nuns, A. S. Mamede, G. Dezanneau, C. Y. Yoo, H. J. M. Bouwmeesterc and R. N. Vannier, *J. Mater. Chem. A*, 2014, **2**(46), 19717–19725.
8 B. Paul, J. L. Schroeder, S. Kerdsongpanya, N. V. Nong, N. Schell, D. Ostach, J. Lu, J. Birch and P. Eklund, *Adv. Electron. Mater.*, 2015, **1**, 1400022.
9 B. Paul, J. Lu and P. Eklund, *ACS Appl. Mater. Interfaces*, 2017, **9**, 25308–25316.
10 B. Paul, E. M. Björk, A. Kumar, J. Lu and P. Eklund, *ACS Appl. Energy Mater.*, 2018, **1**, 2261–2268.
11 Y. Du, J. Xu, B. Paul and P. Eklund, *Appl Mater Today*, 2018, **12**, 366–388.
12 T. Kanno, S. Yotsuhashi and H. Adachi, *Appl. Phys. Lett.*, 2004, **85**, 739.
13 B. Paul, J. Lu and P. Eklund, *Nanomaterials*, 2019, **3**, 443.
14 S. Jo, S. Choo, F. Kim, S. H. Heo and J. S. Son, *Adv. Mater.*, 2018, 1804930.
15 Z. Wang, Y. Ma, P. B. Vartak and R. Y. Wang, *Chem. Commun.*, 2018, **54**(65), 9055–9058.
16 A. L. Tiano, C. Koenigsmann, A. C. Santulli and S. S. Wong, *Chem. Commun.*, 2010, **46**(43), 8093–8130.
17 R. Wei, X. Tang, J. Yang, J. Dai, C. Liang, W. Song, X. Zhu and Y. Sun, *J. Am. Ceram. Soc.*, 2013, **96**, 2396–2401.
18 R. Moubah, S. Colis, C. Leuvrey, G. Schmerber, M. Drillon and A. Dinia, *Thin Solid Films*, 2010, **518**, 4546–4548.
19 L. S. Panchakarla, L. Lajaunie, A. Ramasubramaniam, R. Arenal and R. Tenne, *ACS Nano*, 2016, **10**, 6248–6256.
20 B. Rivas-Murias, J. M. Vila-Fungueiriño and F. Rivadulla, *Sci. Rep.*, 2015, **5**, 11889.
21 R. S. Lanigan and T. A. Yamarik, *Int. J. Toxicol.*, 2002, **21**, 95–142.
22 H. Okada, *In Colloid and Interface Science in Pharmaceutical Research and Development*, Elsivier, 2014, 347–368.
23 J. Liu, X. Huang, F. Li, R. Liu and L. Chen, *J. Phys. Soc. Jpn.*, 2011, **80**, 074802.
24 J. Liu, X. Huang, G. Xu and L. Chen, *J. Alloys Comp.*, 2013, **576**, 247–249.
25 K. Knížek, Z. Jirák, J. Hejtmánek, M. Maryško and J. Buršík, *J. Appl. Phys.*, 2012, **111**, 07D707.
26 W. Liu, H. S. Kim, Q. Jie and Z. Ren, *Scr. Mater.*, 2016, **111**, 3–9.
27 C. Morales, E. Flores, J. R. Ares, C. Sánchez and I. J. Ferrer, *Phys. Status Solidi RRL*, 2018, **12**, 1800277.
28 O. Clement, B. M. Rapko and B. P. Hay, *Coord. Chem. Rev.*, 1998, **170**, 203–243.
29 C. P. Li and M. Du, *Chem. Commun.*, 2011, **47**(21), 5958–5972.
30 S. Garain, T. K. Sinha, P. Adhikary, K. Henkel, S. Sen, S. Ram, C. Sinha, D. Schmeißer and D. Mandal, *ACS Appl. Mater. Interfaces*, 2015, **7**, 1298–1307.
31 A. Lan, K. Li, H. Wu, D. H. Olson, T. J. Emge, W. Ki, M. Hong and J. Li, *Angew. Chem.*, 2009, **121**, 2370–2374.
32 P. Saarinen-Savolainen, T. Järvinen, K. Araki-Sasaki, H. Watanabe and A. Urtti, *Pharm. Res.*, 1998, **15**, 1275–1280.
33 Y. Bitla and Y.-H. Chu, *FlatChem*, 2017, **3**, 26–42.
34 E. Bonaccurso, M. Kappl and H. J. Butt, *Phys. Rev. Lett.*, 2002, **88**, 076103.
35 I. Pastoriza-Santos and L. M. Liz-Marzán, *Adv. Funct. Mater.*, 2009, **19**, 679–688.
36 R. K. Chowdhury, T. K. Sinha, A. K. Katiyar and S. K. Ray, *Nanoscale*, 2017, **9**, 15591–15597.
37 B. L. Cushing and J. B. Wiley, *J. Solid State Chem.*, 1998, **141**, 385–391.
38 X. Zhu, D. Shi, S. Dou, Y. Sun, Q. Li, L. Wang, W. Li, W. Yeoh, R. Zheng, Z. Chen and C. Kong, *Acta Mater.*, 2010, **58**, 4281–4291.
39 J. P. Cheng, X. Chen, J. S. Wu, F. Liu, X. B. Zhang and V. P. Dravid, *CrystEngComm*, 2012, **14**, 6702–6709.
40 Y. Q. Guo, J. L. Luo, D. Wu, Z. Li, N. L. Wang and D. Jin, *Phys. Rev. B: Condens. Matter Mater. Phys.*, 2007, **75**, 214432.
41 H. P. An, C. H. Zhu, W. W. Ge, Z. Z. Li and G. D. Tang, *Thin Solid Films*, 2013, **545**, 229–233.
42 M.-G. Kang, K.-H. Cho, S.-M. Oh, J.-S. Kim, C.-Y. Kang, S. Nahm and S.-J. Yoon, *Appl. Phys. Lett.*, 2011, **98**, 142102.
43 R. Benoit, V. Hornebecq, F. Weill, L. Lecren, X. Bourrat and M. Tréguer-Delapierre, *J. Mater. Chem. A*, 2013, **1**(45), 14221–14226.
44 M. R. Wagner, B. Graczykowski, J. S. Reparaz, A. El Sachat, M. Sledzinska, F. Alzina and C. M. Sotomayor Torres, *Nano Lett.*, 2016, **16**, 5661–5668.